

# Large-deviation properties of the largest biconnected component for random graphs

Hendrik Schawe<sup>a</sup> and Alexander K. Hartmann<sup>b</sup>

Institut für Physik, Universität Oldenburg, 26111 Oldenburg, Germany

January 30, 2019

**Abstract.** We study the size of the largest biconnected components in sparse Erdős-Rényi graphs with finite connectivity and Barabási-Albert graphs with non-integer mean degree. Using a statistical-mechanics inspired Monte Carlo approach we obtain numerically the distributions for different sets of parameters over almost their whole support, especially down to the rare-event tails with probabilities far less than  $10^{-100}$ . This enables us to observe a qualitative difference in the behavior of the size of the largest biconnected component and the largest 2-core in the region of very small components, which is unreachable using simple sampling methods. Also, we observe a convergence to a rate function even for small sizes, which is a hint that the large deviation principle holds for these distributions.

**PACS.** XX.XX.XX No PACS code given

## 1 Introduction

The robustness of networks [1–5] attracted much interest in recent time, from practical applications for, e.g., power grids [6–8], the internet [9,10], to examinations of genomes [11,12]. As typical in network science, one does not only study the properties of existing networks. To model the properties of real networks, different ensembles of random graphs were devised, e.g., Erdős-Rényi random graphs [13], small world graphs [14], or scale-free graphs [15]. Also for such ensembles the robustness has been studied by analytical and numerical means [16–19]. One often used approach to determine the robustness of networks are *fragmentation* studies, where single nodes are removed from the network. These nodes are selected according to specific rules (“attack”) or randomly (“failure”). The functionality, e.g., whether it is still connected, is tested afterwards. It has been suggested that the large deviations are of interest to network robustness, e.g., for the size of the giant connected component, rare configurations of the realization of the damage to networks may change the typically continuous phase transition to a discontinuous phase transition [20,21]. A property necessary for robustness is thus that the graph stays connected when removing an arbitrary node. This exact concept is characterized by the *biconnected component*, which are the connected components which stay connected after an arbitrary node is removed. The existence of a large biconnected component is thus a simple and fundamental property of a graph robust to fragmentation. Another, though

related, often studied form of stability looks at the flow through or the transport capability [10] of a graph. Also here a large biconnected component is a good indicator for stability. Intuitively, in a biconnected component there is never a single bottleneck but always a backup path to reach any node. This ensures the function of the network even in case that an arbitrary edge has too low throughput or an arbitrary node of the biconnected component is damaged.

At the same time, the biconnected component is a simple concept enabling to some extent its treatment by analytical means for some graph ensembles. For example, the mean size  $\langle S_2 \rangle$  of the biconnected component for a graph with a given degree distribution is known [18]. Also, the percolation transition of the biconnected component for scale-free and Erdős-Rényi graphs is known to coincide with the percolation transition of the single connected component, and its finite size scaling behavior is known [22]. Nevertheless, a full description of any random variable is only obtained if its full probability distribution is known. To our knowledge, concerning the size of the biconnected component this has not been achieved so far for any graph ensemble, neither analytically nor numerically.

For few network observables and some graph ensembles results concerning the probability distributions have been already obtained so far. For the size of the connected component on Erdős-Rényi random graphs analytical results [23] for the rate function exist, i.e., the behavior of the full distribution for large graph sizes  $N$ . Numerically it was shown that this is already for relatively small  $N$  a very good approximation [24]. Corresponding numerical results for two-dimensional percolation have been ob-

<sup>a</sup> Present address: hendrik.schawe@uni-oldenburg.de

<sup>b</sup> Present address: a.hartmann@uni-oldenburg.de

tained as well [24]. Similarly there are numerical, but no analytical works, scrutinizing the size of the related 2-core over most of its support again for Erdős-Rényi random graphs [25].

Since similar results seem not to be available concerning the biconnected components, and given its importance for network robustness, this is an omission that we will start to cure with this study. Here, we numerically [26] obtain the probability density function of the size of the largest biconnected component over a large part of its support, i.e., down to probabilities smaller than  $10^{-100}$ . This enables us also to directly observe large deviation properties, and shows strong hints that the large deviation principle holds [27, 28] for this distribution.

The remainder of this manuscript gives definitions of the graph ensembles and the properties of interest, as well as some known results, in section 2.1 and explains the sampling methods needed to explore the tails of the distributions in section 2.2. The results of our simulations and a discussion will follow in section 3. Section 4 summarizes the results.

## 2 Models and Methods

### 2.1 Biconnected Components of Random Graphs

A *graph*  $G = (V, E)$  is a tuple of a set of nodes  $V$  and edges  $E \subset V^{(2)}$ . A pair of nodes  $i, j$  are called *connected*, if there exists a *path* of edges  $\{i, i_1\}, \{i_1, i_2\}, \dots, \{i_{k-1}, i_k\}, \{i_k, j\}$  between them. A *cycle* is a closed path, i.e., the edge  $\{i, j\}$  exists and  $i$  and  $j$  are connected in  $G' = (V, E \setminus \{i, j\})$ . The *connected components* are the maximal disjoint subgraphs, such that all nodes of each subgraph are connected.

A *biconnected component* (sometimes *bicomponent*) of an undirected graph is a subgraph, such that every node can be reached by two paths, which are distinct in every node except the start- and end node. Thus, if any single node is removed from a biconnected component it will still be a connected component. Therefore clearly, each biconnected component is a connected component. We will also look shortly at *bi-edge-connected components*, which are very similar, but the two paths may share nodes as long as they do not share any edge. Note that a biconnected component is always a bi-edge-connected component, but the reverse is not necessarily true. An example is shown in Fig. 1. In this study we will study mainly the largest biconnected component  $G_{\text{bi}}$ . Note that, while every biconnected component is also a connected component, the largest biconnected component does not need to be a subgraph of the largest connected component  $G_{\text{cc}}$ , it may be part of another, smaller, connected component. However, its size  $S_2 = |G_{\text{bi}}|$  is always smaller or equal than the size of the largest connected component  $S = |G_{\text{cc}}|$ . Similarly, the size  $S_{2\text{-core}}$  of the largest connected component of the 2-core, the subgraphs that remain after iterative removal of all nodes with degree less than 2, is an upper bound on  $S_2$ , since the 2-core of a graph consists of bicomponents possibly linked by single edges. In Fig. 1 the largest

components of each type are visualized for an example connected graph. In fact for the sizes of the largest of the above introduced subgraphs, the following relation holds.

$$S \geq S_{2\text{-core}} \geq S_{2\text{-edge}} \geq S_2. \quad (1)$$

As we will see below, for the ensemble of Erdős-Rényi random graphs in the percolating phase, the distributions of  $S_{2\text{-core}}$ ,  $S_{2\text{-edge}}$ , and  $S_2$  are actually very similar to each other. One has indeed to inspect the far tails of the distributions to see differences, which also justifies that we study the large-deviation properties here. For the ensemble of Barabási-Albert graphs we study, the same is true. While the distributions of  $S_{2\text{-core}}$  and  $S_2$  look very similar in the main region, a qualitative difference is observable in the tail of small components. The difference is even more pronounced than for the ER case, since the general form of the distribution changes qualitatively to a convex shape for  $P(S_{2\text{-core}})$ .

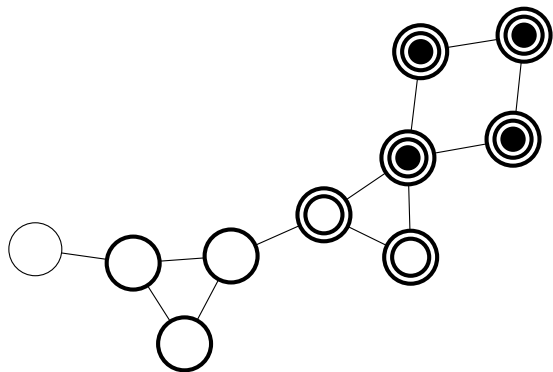


**Fig. 1.** Every node is part of the connected component, nine nodes with bold borderline are part of the 2-core, six nodes containing a circle are part of the largest bi-edge-connected component and all nodes containing a black dot are part of the largest biconnected component.

The classical way to find biconnected components of a graph [29] is based on a depth first search and thus runs in linear time. For each connected component a depth first search is started at an arbitrary root node of that component. For each node the current *depth* of the search, i.e., at which level in the tree traversed by the depth first search the node is located, and the *lowpoint* are saved. The lowpoint is the minimum of the depth of the neighbors (in the graph) of all descendants of the node (in the tree). If the depth of a node is less or equal the lowpoint of one of its children (in the tree), this node separates two biconnected components and is called *articulation point*. For the root node of the search there is an exception. It is an articulation point, iff it has more than one child. The articulation points separate biconnected components and are members of all biconnected components separated by them. A better illustrated explanation can be found in [30]. After finding all biconnected components, we measure the size of the largest. We used the efficient implementation of this algorithm provided by the LEMON graph library [31].

The mean size of the biconnected component of graphs with a given degree distribution  $p_k$  is known for large graphs [18,32] to be

$$\langle S_2 \rangle = 1 - G_0(u) - (1-u)G'_0(u), \quad (2)$$

where  $G_0(z) = \sum_k p_k z^k$  is the probability generating function,  $G'_0$  its derivative and  $u$  the probability to reach a node not part of the giant connected component when following an edge.  $u$  is determined by the solution of

$$u = \sum_{k=0}^{\infty} q_k u^k, \quad (3)$$

with the excess degree distribution  $q_k = (k+1)p_{k+1}/\langle k \rangle$ . Knowing the degree distribution of Erdős-Rényi graphs  $G(N, p)$  to be

$$p_k = \binom{N-1}{k} p^k (1-p)^{N-1-k}, \quad (4)$$

allows the numerical evaluation of Eq. (3). We will compare these predictions to our simulational results to scrutinize the behavior for finite  $N$ .

The ensemble of *Erdős-Rényi* (ER) graphs  $G(N, p)$  consists of  $N$  nodes and each of the  $N(N-1)/2$  possible edges occurs with probability  $p$ . The connectivity  $c = Np$  is the average number of incident edges per node, the average *degree*. At  $c_c = 1$  this ensemble shows a *percolation transition*. That is in the limit of large graph sizes  $N$  the size of the largest connected component is of order  $\mathcal{O}(N)$  above this threshold and of order  $\mathcal{O}(1)$  below. Interestingly this point is also the percolation transition of the biconnected component [22].

To a lesser extend we also study *Barabási-Albert* (BA) graphs [15]. The ensemble of BA graphs is characterized by a tunable mean degree  $\langle k \rangle$  and its degree distribution follows a powerlaw  $p(k) \propto k^{-3}$ . Realizations are constructed using a growth process. Starting from a fully connected subgraph of  $m_0$  (here  $m_0 = 3$ ) nodes, in every iteration one more node is added and connected to  $m \leq m_0$  existing nodes  $j$  with a probability  $p_j \propto k_j$  dependent on their degree  $k_j$  until the size of the graph is  $N$ . The parameter  $2m = \langle k \rangle$  by construction. Since  $m = 1$  will always result in a tree, which is not biconnected at all and  $m \geq 2$  will always be a full biconnected component, we will allow fractional  $1 < m < 2$  in the sense, that one edge is always added and a second with probability  $m - 1$ .

We also take a brief look at the *configuration model* (CM) [33], an ensemble of graphs constructed to follow an arbitrary degree distribution. To sample the space of all simple graphs, i.e., graphs without self-loops and multi-edges, of the configuration model, one has to generate first a random degree distribution, add stubs to the nodes according to the degree distribution, connect the stubs randomly and start from scratch in the case that the result is not a simple graph [34]. This means, the amount of random numbers needed to generate one instance of a CM graph will vary, sometimes very strongly, if the instances are “difficult” to construct.

## 2.2 Sampling

Since we are interested in the far tail behavior of the distribution of the size of the largest biconnected component, it is infeasible to use naive simple sampling, i.e., uniformly generating configurations, measuring the observable and constructing a histogram. Instead we use a Markov chain Monte Carlo based importance sampling scheme to collect good statistics also in the far tails. This technique was already applied to obtain the distributions over a large range for the score of sequence alignments [35–37], to obtain statistics of the convex hulls of a wide range of types of random walks [38–41], to work distributions for non-equilibrium systems [42] and especially to different properties of Erdős-Rényi random graphs [43,24,25,44].

The Markov chain in this case is a chain of random number vectors  $\xi_t$ ,  $t = 1, 2, \dots$ . Each entry of  $\xi_t$  is drawn from a uniform  $U(0, 1)$  distribution. Each vector serves as an input for a function which generates a random graph. Since all randomness is included in  $\xi_t$ , the generated graph  $G_t = G(\xi_t)$  depends deterministically on  $\xi_t$ . In this way, the Markov chain  $\{\xi_t\}$  corresponds to a Markov chain  $\{G_t\}$  of graphs. This approach, of separating the randomness from the actually generated objects, has the advantage that for the Markov chain we can generate graph realizations of arbitrary ensembles from scratch, without having to invent a valid Markov chain change move for each ensemble. However, for Erdős-Rényi graphs, we use a specialized change move for performance reasons. One change move is to select a random node  $i$ , delete all incident edges and add every edge  $\{i, j\}$  with  $j \in V \setminus \{i\}$  with probability  $p$ . For the Barabási-Albert graphs such a simple change move is not trivial to construct. Therefore, for this type, we perform the typical growth process from scratch after changing one of the underlying random numbers in  $\xi_t$ .

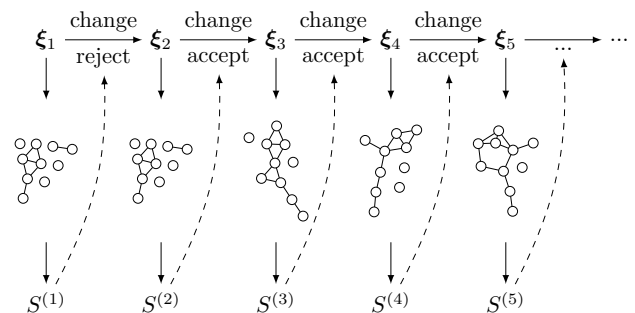


**Fig. 2.** Four steps of our importance sampling scheme at a small negative temperature, biasing towards a larger biconnected component.

The main idea to obtain good statistics over a large part of the support, especially for probabilities smaller than, say,  $10^{-100}$ , is to bias the generated samples towards those regions. Therefore, we will use classical Metropolis sampling to gather realizations of graphs  $G$ . The Markov chain underlying this method consists of either Graph realizations  $G$  (ER case) or random number vectors  $\xi$  from

which a graph realization can be constructed  $G(\xi)$  (BA case). We will describe the process for the latter more general case. We start our Markov chain with some random state  $\xi_1$  and at every iteration we propose a new state  $\xi'$ , i.e., replace a single entry of  $\xi_t$  with a new uniform random number and generate a new realization  $G(\xi')$  from these random numbers. We will accept this proposal as the new state  $\xi_{t+1}$ , with the classical Metropolis acceptance probability  $p_{\text{acc}} = \min\{1, e^{-\Delta S/T}\}$ . This process is sketched in Fig. 2. Since we are interested in the size of the largest biconnected component  $S$ , we will treat this observable as the “energy” of the realization. Thus,  $\Delta S$  is the difference in energy between the old and proposed state. Otherwise the proposal is rejected, i.e.,  $\xi_{t+1} = \xi_t$ . Following this protocol, the Markov chain will equilibrate eventually and from thereon yield realizations  $G(\xi)$  which are Boltzmann distributed with respect to some “artificial temperature”  $T$

$$Q_T(G) = \frac{1}{Z_T} e^{-S(G)/T} Q(G), \quad (5)$$

where  $Q(G)$  is the natural distribution of the realizations and  $Z_T$  the partition function, i.e., a normalization constant. Now, we can use the temperature  $T$  as a tuning parameter to adjust the part of the distribution we want to gather samples from. Low positive temperatures will bias the “energy”  $S$  towards smaller values because decreases in  $S$  are always accepted and increases in  $S$  are more often rejected. For negative  $T$  this bias works in the opposite way towards larger values of  $S$ , i.e., larger biconnected components in this case.

Note that, while this scheme is generally applicable to any model, there are models which are infeasible to equilibrate. As an example take the configuration model. The above described construction poses the problem that we use two types of random numbers. The first  $N$  random numbers to generate a degree distribution  $p_k$  and the remainder  $\sum_{k=1}^{N-1} k p_k$  for the connections between the stubs. Thus, the amount of random number varies somehow. But this is true only if in the first attempt a valid set of edges is created. If not, one would need to perform for the current degree sequence one or several other attempts, creating the need for many more random numbers. Thus, a state  $\xi$  of the random numbers would be much larger, containing many numbers “in stock”, much larger than needed to construct a typical graph which requires only one attempt. First, this makes in somehow numerically demanding. But even worse, in total this mean that a small change to one of the first  $N$  random numbers typically leads to a strong change of the resulting graph, such that almost all changes of this kind will be rejected when approaching the tails. It might, of course, be possible to devise an efficient change move. Nevertheless, we were not able to sample the biconnected component of the configuration model in the far tails, and will only use data obtained by simple sampling for some qualitative comparisons of the three graph ensembles.

For any chosen temperature, the sampling will be restricted to some interval determined by the value of  $T$ .

Thus, to obtain the desired distribution  $P(S)$  over a large range of the support, simulations for many different temperatures have to be performed. We have to choose the temperatures  $T$  in a certain way, to be able to reconstruct the wanted distribution  $P(S)$  from this data. First, we can transform  $Q(G)$  into  $P(S)$  by summing all realizations  $G$ , which have the same  $S$ . Hence we obtain with Eq. (5)

$$\begin{aligned} P_T(S) &= \sum_{\{G|S(G)=S\}} Q_T(G) \\ &= \sum_{\{G|S(G)=S\}} \frac{\exp(-S/T)}{Z_T} Q(G) \\ &= \frac{\exp(-S/T)}{Z_T} P(S). \end{aligned}$$

With this relation we can calculate the wanted, unbiased distribution  $P(S)$  from measurements of our biased distributions  $P_T(S)$ . The ratios of all constants  $Z_T$  can be obtained by enforcing continuity of the distribution  $P(S)$ , i.e.,

$$P_{T_j}(S) e^{S/T_j} Z_{T_j} = P_{T_i}(S) e^{S/T_i} Z_{T_i}.$$

This requires that our measurements for  $P_T(S)$  are at least pairwise overlapping such that there is no unsampled region between sampled regions. From pairwise overlaps the pairwise ratios  $Z_i/Z_j$  can be approximated. The absolute value of the  $Z_T$  can afterwards be obtained by the normalization of  $P(S)$ . Although the size of the largest biconnected component  $S_2$  is a discrete variable for every finite  $N$  and should therefore be normalized such that the probabilities of every event should sum to one, i.e.,  $\sum_{i=0}^N p(S_2 = i/N) = 1$ , we are mainly interested in the large  $N$  behavior and especially the rate function. This limit is continuous and should therefore be treated with a different normalization  $\int_0^1 p(S_2) dS_2 = 1$ , which we approximate for finite  $N$  by the trapezoidal rule. Anyway, the difference here is just a factor  $N$ .

While this technique does usually work quite well and all distributions but one exception are obtained with this method, there are sometimes first order phase transitions within the finite temperature ensemble, rendering it infeasible, or at least very tedious, to acquire values inbetween two temperatures. This was a problem here for the modified Barabási-Albert graph at the largest simulated graph size  $N$ . This phenomenon is well known and explored in detail in [24]. We filled this gap by modified Wang-Landau simulations [45–49] with subsequent entropic sampling [50, 51].

### 3 Results

We applied the temperature-based sampling scheme to ER with finite connectivities of  $c \in \{0.5, 1, 2\}$  and BA with  $m = 1.3$  over practically the whole support  $S_2 \in [0, 1]$  using around a dozen different temperatures for each ensemble and Markov chains of length  $10^6 N$  to gather enough

samples after equilibration and discarding correlated samples. Additionally for BA the range  $S_2 \in [0.1, 0.35]$  was sampled using Wang-Landau's method and merged into results obtained from the temperature based sampling for the remainder of the distribution. All error estimates for the distributions are obtained via bootstrap resampling [52, 53] but are always smaller than the symbol size and therefore not shown. Error estimates for fit parameters are Gnuplot's asymptotic standard errors corrected according to Ref. [53].

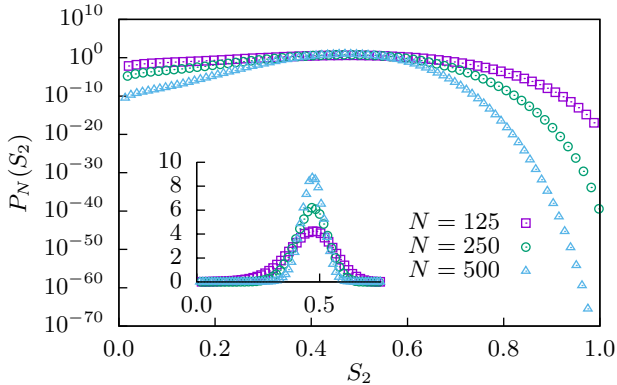


**Fig. 3.** Distributions of the size of the largest biconnected component  $S_2$  for ER graphs at connectivity  $c = 2$  and three different graph sizes  $N$ . The main plot shows the distributions in logarithmic scale to display the tails, the inset shows the same distributions in linear scale, where a concentration around the mean value  $\langle S_2 \rangle$  (cf. Fig 4) is visible. Note that despite  $P_N(S_2)$  being a discrete distribution, it is normalized like a continuous distribution (see second to last paragraph of the methods section for the rationale). (For clarity not every bin is visualized.)

Examples for the distribution of the largest biconnected component's size for ER graphs at  $c = 2$  are depicted in Fig. 3 at three different graph sizes  $N$ . The inset shows the distribution in linear scale, where a concentration with increasing size  $N$  around the mean value is visible. While the main part of the distribution in the inset looks rather symmetric, the tails are obviously not. Also it is visible that the tails of the distribution get more and more suppressed when increasing the value of  $N$ .

Since the mean size of the biconnected component of ER is known for large enough graphs, we will compare the mean sizes of our simulations to the analytical expectation. Those results are shown in Fig. 4, notice the broken  $\langle S_2 \rangle$ -axis. Apparently at  $c = 2$  for small sizes  $N$  the analytical approximation, while close to our measurements, overestimates the size of the biconnected component slightly but the relative error diminishes for larger sizes. In fact, we extrapolated our measurements to the limit of large  $N$  using a power-law ansatz  $\langle S_2 \rangle = aN^b + S_2^\infty$  yielding for  $c = 0.5$  an offset  $S_2^\infty$  compatible within errorbars with the expectation  $\langle S_2 \rangle = 0$  (exact values in the caption of Fig. 4), which is quite remarkable for our ad-hoc fit function. The case  $c = 1$  suggests a negative  $S_2^\infty$  close

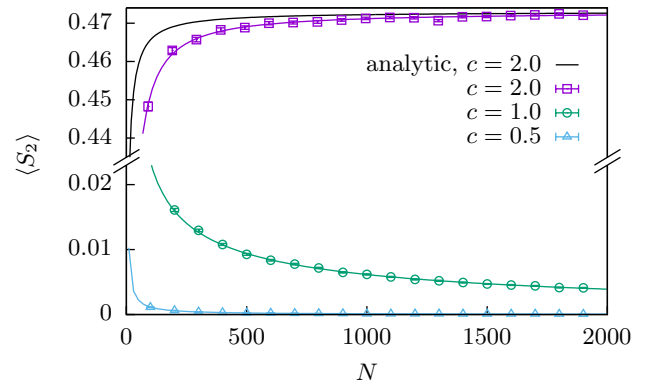


**Fig. 4.** Mean size of the largest biconnected component  $\langle S_2 \rangle$  for different graph sizes  $N$ . Notice the broken  $\langle S_2 \rangle$ -axis. The black line denotes the analytic expectation for  $c = 2$  from Eq. (2) [18]. The expectation for  $c \leq 1$  is  $\langle S_2 \rangle = 0$ . Fits to a power law with offset  $\langle S_2 \rangle = aN^b + S_2^\infty$  lead to  $S_2^\infty = -6(8) \cdot 10^{-6}$  for  $c = 0.5$ ,  $S_2^\infty = -0.0013(4)$  for  $c = 1$  and  $S_2^\infty = 0.4729(3)$  for  $c = 2$ .

to zero, which is probably caused by correction to our assumed scaling law. The case  $c = 2$  seems to converge to the limit of the analytical expectation also.

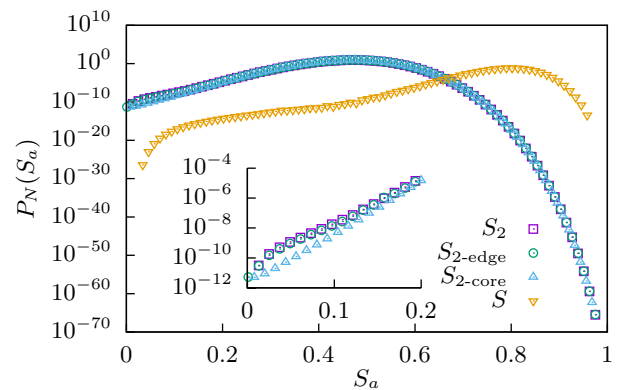


**Fig. 5.** Comparison of the relative sizes  $S_a$ , which can be any of the largest connected component  $S$  [24], the largest 2-core  $S_{2\text{-core}}$  [25], the largest bi-edge-connected component  $S_{2\text{-edge}}$  and the largest biconnected component  $S_2$  for  $N = 500$  and  $c = 2$  ER graphs. The last three are nearly identical for sizes  $S_a \gtrsim 0.2$ . The inset shows a zoom to the very small components, which is the only region, where the three last types deviate considerably from one another. For clarity not every data point is visualized.

To compare the sizes of different relevant types of components, Fig. 5 shows the distributions of the relative size of the largest connected component  $S$  [24], the largest 2-core  $S_{2\text{-core}}$  [25], the largest bi-edge-connected component  $S_{2\text{-edge}}$  and the largest biconnected component  $S_2$  for  $N = 500$  and  $c = 2$  ER graphs. Interestingly, the distributions  $P_N(S_2)$ ,  $P_N(S_{2\text{-edge}})$  and  $P_N(S_{2\text{-core}})$  are almost identical and only deviate in the region of very small components from each other. As would be expected by the

order of Eq. (1), the probability to find very small 2-cores is lower than to find bi-edge-connected components of the same small size, which are again slightly less probable than biconnected components of that size. Anyway, when considering ER graphs, which exhibit by construction no particular structure, the robustness properties which are determined by the biconnected component, can be with very high probability readily inferred from the 2-core.

To understand the reason for the sizes  $S_2$ ,  $S_{2\text{-edge}}$  and  $S_{2\text{-core}}$  to be so similar for graphs with independently created edges like ER and CM, consider the argumentation of Ref. [18], where an upper bound Eq. (2), which becomes exact for  $N \rightarrow \infty$ , is derived as the probability of a node to have two edges connecting to the giant component. For finite graphs this is just an upper bound, as two paths to the giant component are necessary for a node to be part of the giant biconnected component but not sufficient. To be sufficient, we have to ensure that the two paths do not share any nodes (or any edges for the bi-edge-connected component). Similarly, this criterion also works for the giant 2-core in the limit of large  $N$ , but here it does not provide an upper bound, because two independent paths are not necessary. For a node to not be a leaf at some point in the process of finding a 2-core, it has to be connected with two edges to other biconnected components, possibly the same. To be part of the giant two core it has to be in the connected component. Using the argumentation of Ref. [18] that small biconnected components are very rare for large values of  $N$ , we see that the two biconnected components with which any node of the giant 2-core is connected are with high probability just part of the giant biconnected component. One would therefore expect that in the  $N \rightarrow \infty$  case these observables behave the same. And indeed, in our data we observe that the regime where they behave most differently is in graphs with atypically small sizes of the components, again highlighting the power of the large-deviation approach without which it would be impossible to observe these differences. Keep in mind that this argument does only work for models with independently placed edges, like the ER or CM models. Indeed we will see below that for the BA model, the differences between the component types are much larger.

To understand the topology of the instances of very low probabilities better, we will look at the correlations of the size of the largest connected component  $S$  and the largest biconnected component in Fig. 6. Note that this histogram does not reflect the probabilities, but does count the instances we generated within one of our simulations, i.e., data for many different temperatures are shown without correction for the introduced bias. Anyway, it is instructive to look at this sketch for qualitative understanding. This data is for  $c = 2$  ER at  $N = 500$ . We observe that, even for our biased sampling, there are basically no large biconnected components if the connected component is smaller than  $S \lesssim 0.6$ . Above this point, we observe larger biconnected components, but generally very few around the size  $S_2 \approx 0.2$ . Above  $S \gtrsim 0.6$  the size of the largest bi-

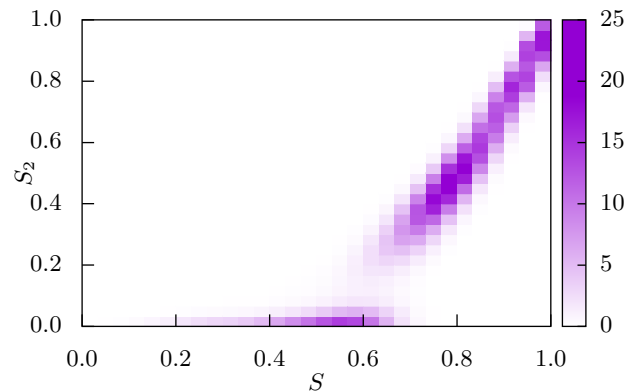


**Fig. 6.** Correlation histogram of our raw and biased simulation data for the  $c = 2$  ensemble of ER graphs. A large biconnected component does most probably appear in graphs whose connected component is larger than  $S \gtrsim 0.6$ . This is a qualitative correlation plot only, as the exact values of the bins are dependent on the temperatures used for the simulation. The colorbar encodes a normalized probability density to encounter the corresponding pair of values in our finite-temperature ensembles.

connected component is strongly correlated with the size of the largest connected component.

For a qualitative understanding of this behavior, consider the following heuristic argument. For the instances without or with very small biconnected components, i.e., only short cycles, the graph is basically tree-like. Larger biconnected components are then created by connecting two nodes of the tree with each other, leading to a cycle which is on average in the order of the size of the tree, leading to the jump in the size of biconnected components. The configurations with smaller biconnected components are apparently entropically suppressed.

Next we will look at the empirical large deviation *rate function* of the measured distributions. The rate function  $\Phi$  describes the behavior of distributions, whose probability density decays exponentially in the tails in respect to some parameter  $N$ . In this case, the parameter  $N$  is the graph size. For increasing graph size  $N$  the biconnected components which are not typical will be exponentially suppressed. To be more precise, the definition of the rate function  $\Phi(S_2) \geq 0$  is via  $P_N(S_2) = e^{-N\Phi(S_2) + o(N)}$  for the large  $N$  limit with the Landau symbol  $o(N)$  for terms of order less than  $N$ . If a rate function exists, we can read off, for example, that the value  $S_2^*$  at which the rate function  $\Phi(S_2^*) = 0$  is the value around which the probability concentrates, i.e., the size of the biconnected component is self averaging.

Since we obtained the distributions  $P_N$  over most of their support but at finite  $N$ , we can only access the *empirical rate function*  $\Phi_N$  for finite values of  $N$ , i.e.,

$$\Phi_N(S_2) = -1/N \log P_N(S_2) + o(N)/N. \quad (6)$$

Note also that the empirical rate functions do contain all information of the measured distributions  $P_N$ , such that we will only visualize either  $P_N$  or  $\Phi_N$  in the following.

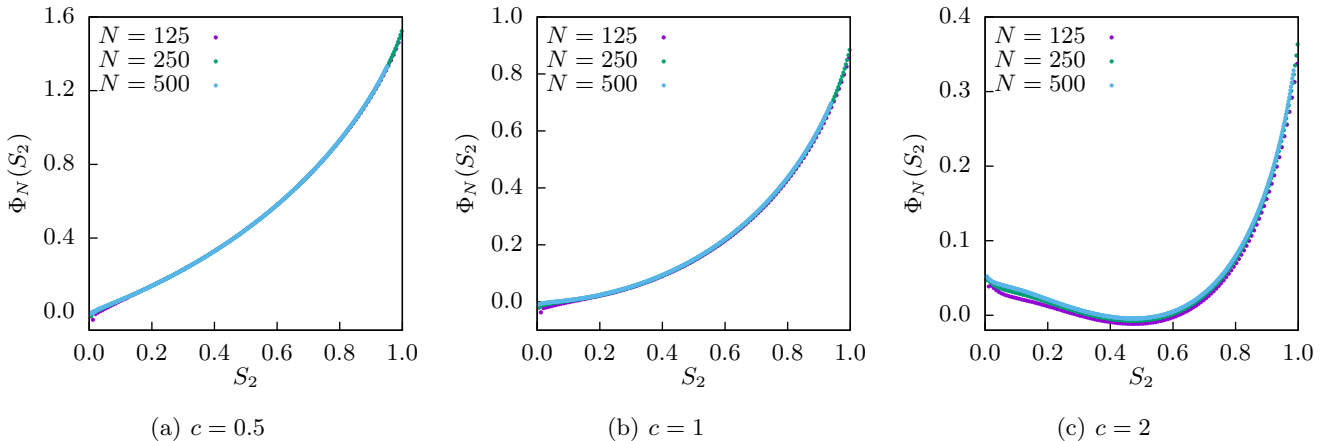


**Fig. 7.** Empirical rate function  $\Phi_N(S_2)$  for multiple graph sizes  $N$  and connectivities  $c$  of the ER graph ensemble. (a) below the percolation transition, (b) at the percolation transition and (c) above the percolation transition. For the cases (a) and (b) finite size effects are minor and a very fast convergence towards the rate function valid for large values of  $N$  is visible. The case (c) shows a qualitatively different behavior, where the minimum of the empirical rate function is shifted to finite values. The convergence towards the actual rate function is visible.

Note also that the  $o(N)$  term leaves enough freedom at finite  $N$  to shift the empirical rate function a bit such that negative values can occur. However, if for increasing values of  $N$  a convergence to a limiting curve is visible, this limiting curve is the actual rate function and one says the distribution follows the *large deviation principle* [27, 28].

In Fig. 7 the empirical rate functions for ER at different connectivities  $c$  and for different sizes  $N$  are shown. The data of the distribution has a very high precision as the values of the rate function  $\Phi_{500}$  in the case 7(a) reaches values of  $\Phi_{500} = 1.5$  corresponding to probabilities less than  $10^{-300}$ . Already these comparatively small values of  $N$  show remarkably similar empiric rate functions and strongly hint at a convergence to a limit form. Also, while near the minima negative values of the empirical rate function occur, it is clear that the convergence is towards zero at those positions, such that it is plausible that the actual rate function is non-negative. While the empirical rate functions in the right tail for larger than typical components  $S_2$  are already almost indistinguishable, the convergence seems a bit slower in the left tail of smaller than typical components. This behavior is very similar to the behavior of the sizes of the connected component [24] and the 2-core [25]. This means that, the large deviation principle seems to hold for this distribution.

Let us now take a look at the BA model. First, we will just compare the mean size of the biconnected component  $\langle S_2 \rangle$ , which we measured on the BA model similar to the extrapolation in Fig. 4 ( $300 \leq N \leq 1000$ ), resulting in  $\langle S_2^{\text{BA}} \rangle \approx 0.4982(4)$  for large values of  $N$ . In comparison to the analytical value  $\langle S_2^{\text{ER}} \rangle = 0.6811\dots$  for large  $N$  [18] for the ER graph with the same mean degree  $\langle k \rangle = 2.6$ , we observe that the connectedness and robustness against random failures of the BA has to be paid with a decreased robustness against worst case failures, which is a phe-

nomenon observed before [16]. To check whether this effect is caused by the degree distribution or the correlations, we look at the configuration model with a similar degree distribution, namely a Pareto distribution  $p(k) = 2k_0k^{-3}$  with the same exponent as for the BA model and with a tunable minimum  $k_0$ , which we change to result in a mean degree of  $\langle k \rangle \approx 2.6$ . Note that due to the discrete nature of the degree distribution this does not result in a perfect power law, in particular  $p(\lfloor k_0 \rfloor)$  is lower than for a perfect power law, but it should be close enough for our purposes. Here we observe  $\langle S_2^{\text{CM}} \rangle \approx 0.6650(6)$ . This is slightly lower than the value for ER. This small difference between the ER and CM model is also visible when looking at the typical region of the distribution of  $S_2$  as shown in Fig. 8. This indicates that hubs are a cause to destabilize a network against worst-case failures, but considerably a smaller cause than for BA, indicating that the correlations and the forced connectedness of BA graphs lead to less redundancy in the network. Thus, since the behavior of CM and ER is quite similar, and because of the algorithmic complexity we encounter for the CM model, as mentioned above, we proceed with the the large-deviation behavior of the BA model.

The empirical rate function of the largest biconnected component of the BA ensemble at  $m = 1.3$ , i.e., a mean degree of  $\langle k \rangle = 2.6$ , is shown in Fig. 9. The empirical rate function and therefore the distribution does look qualitatively similar to the  $c = 2$  case of the ER ensemble (cf. Fig. 7(c)). The dip around  $S_2 \approx 0.2$  is more pronounced leading to a more severe discontinuity in the simulated finite temperature ensemble necessitating the use of Wang-Landau sampling. The main qualitative difference of the behavior of the two distributions is visible in the small sizes of the largest biconnected components  $S_2$ , where the empirical rate functions cross each other, hinting at some kind of finite size effect suppressing very small biconnected components in small graphs.

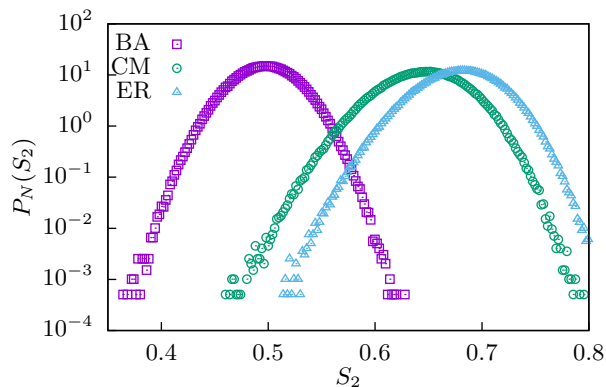


**Fig. 8.** Distribution  $P_N(S_2)$  of the size of the giant biconnected component in the BA model with a mean degree of  $\langle k \rangle = 2.6$  and a power-law degree distribution  $p_k \sim k^{-3}$  in comparison to the CM with approximately the same mean degree and the same exponent governing the power-law degree distribution and the ER model with the same mean degree. Apparently the BA has a far smaller biconnected component than the other two, but is connected. Samples were taken for graphs of size  $N = 500$ .

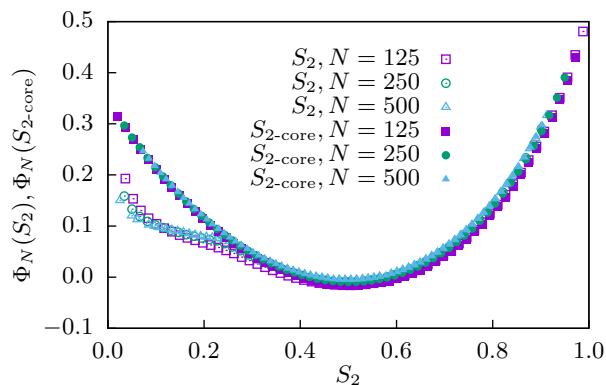


**Fig. 9.** Empirical rate function  $\Phi_N(S_2)$  for multiple graph sizes  $N$  of the BA graph ensemble with  $m = 1.3$ . A convergence towards an asymptotic form for large values of  $N$  is visible. For comparison also the empirical rate function  $\Phi_N(S_2)$  characterizing the distribution of the 2-core is shown. It deviates qualitatively in the far left tail.

In comparison with the empirical rate function of the size of the 2-core  $S_{2\text{-core}}$ , also shown in Fig. 9, their difference in the region of very small bicomponents respectively 2-cores, which was already observable in ER, is very strong in the BA ensemble. Despite those two observables being almost indistinguishable in the main region, they show strongly different behavior in their overall shape, i.e., the distribution of the 2-core seems convex over the region we obtained statistics for. Note however, that in contrast to the ER or even CM with the same degree distribution, we do not expect the two distributions to be indistinguishable in the  $N \rightarrow \infty$  limit. While the argumentation for the ER needed the prerequisite of independent edges, the BA shows strong correlations, e.g., cliques of 3 nodes occur more often than in the ER or a CM with the same

degree distribution. As numerical evidence that the two distributions do not become identical in the  $N \rightarrow \infty$  limit, observe in Fig. 9 that while the 2-core is almost converged already, the left tail of  $\Phi_N(S_2)$  tends away with increasing graph sizes  $N$ . Thus, for infinite graph size, the difference between  $S_2$  and  $S_{2\text{-core}}$  will remain strong and extensive in the left tail.

## 4 Conclusions

The biconnected component is a fundamental observable of any graph related to its robustness. In general, we identified competing properties, which influence the robustness of networks, e.g., while the specific growth process for BA graphs leads to a large connected component, it also leads to a smaller biconnected component. Tests on the configuration model show that the degree distribution has an influence on the size of the biconnected component, but the construction rules of BA graphs have a larger impact. This supports that networks originating from preferential attachment processes might be particularly susceptible to targeted attacks or worst-case failures as compared to networks following the same degree distribution but exhibiting independently drawn edges.

On a more fundamental level, the distribution of its size has not been studied before, to our knowledge. We used sophisticated sampling methods to obtain the distributions of the size of the largest biconnected component  $S_2$ , for multiple ER graph ensembles and a modified BA graph ensemble, over a large part of their support. For the ER ensemble, looking into the large deviation tails of this distribution shows qualitative differences between the size of the 2-core and the biconnected component, which are otherwise not well observable and which we expect to vanish for large systems. Even more interesting is the case for the BA ensemble where the overall shape of the distributions seems to differ also for large systems. While the 2-core distribution seems convex, the distribution of the biconnected component shows a “shoulder”. These qualitative difference, however is only apparent below probabilities of  $10^{-20}$  and are therefore unobservable using conventional methods.

Further, the empirical rate functions are already for the small sizes that we simulated very close to each other hinting at a very fast convergence to the limiting form. Thus, our results indicate that the large deviation principle holds for the numerically obtained distributions. This “well-behaving” of our numerical results may make it promising to address the distribution of the biconnected component by analytical means, which has not been done so far to our knowledge. Furthermore, it would be interesting to study other network ensembles, which are even more relevant for modeling robustness properties, e.g., two-dimensional networks modeling power grids [8] and other transportation networks.

## 5 Acknowledgments

This work was supported by the German Science Foundation (DFG) through the grant HA 3169/8-1. We also thank the GWDG (Göttingen) for providing computational resources.

## 6 Authors contributions

AKH conceived the study, HS wrote the first draft of the manuscript and generated most of the new data. All authors contributed ideas, simulation data and analysis to this study. All authors were involved in the preparation of the manuscript.

## References

1. M.E.J. Newman, *SIAM Review* **45**, 167 (2003)
2. S.N. Dorogovtsev, J.F.F. Mendes, *Evolution of networks: from biological nets to the Internet and WWW* (Oxford Univ. Press, 2006)
3. M. Newman, A.L. Barabási, D. Watts, *The Structure and Dynamics of Networks* (Princeton University Press, 2006)
4. M. Newman, *Networks: an Introduction* (Oxford University Press, 2010)
5. A. Barrat, M. Barthélemy, A. Vespignani, *Dynamical Processes on Complex Networks* (Cambridge University Press, 2012)
6. M.L. Sachtjen, B.A. Carreras, V.E. Lynch, *Phys. Rev. E* **61**, 4877 (2000)
7. M. Rohden, A. Sorge, M. Timme, D. Witthaut, *Phys. Rev. Lett.* **109**, 064101 (2012)
8. T. Dewenter, A.K. Hartmann, *New Journal of Physics* **17**, 015005 (2015)
9. R. Cohen, K. Erez, D. ben Avraham, S. Havlin, *Phys. Rev. Lett.* **85**, 4626 (2000)
10. D.S. Lee, H. Rieger, *EPL (Europhysics Letters)* **73**, 471 (2006)
11. C.M. Ghim, K.I. Goh, B. Kahng, *Journal of Theoretical Biology* **237**, 401 (2005)
12. P. Kim, D.S. Lee, B. Kahng, *Scientific Reports* **5**, 15567 (2015)
13. P. Erdős, A. Rényi, *Publ. Math. Inst. Hungar. Acad. Sci.* **5**, 17 (1960)
14. D.J. Watts, S.H. Strogatz, *Nature* **393**, 440 (1998)
15. A.L. Barabási, R. Albert, *Science* **286**, 509 (1999)
16. R. Albert, H. Jeong, A.L. Barabási, *Nature* **406**, 378 (2000)
17. D.S. Callaway, M.E.J. Newman, S.H. Strogatz, D.J. Watts, *Phys. Rev. Lett.* **85**, 5468 (2000)
18. M.E.J. Newman, G. Ghoshal, *Phys. Rev. Lett.* **100**, 138701 (2008)
19. C. Norrenbrock, O. Melchert, A.K. Hartmann, *Phys. Rev. E* **94**, 062125 (2016)
20. G. Bianconi, *Phys. Rev. E* **97**, 022314 (2018)
21. G. Bianconi, *Phys. Rev. E* **96**, 012302 (2017)
22. P. Kim, D.S. Lee, B. Kahng, *Phys. Rev. E* **87**, 022804 (2013)
23. M. Biskup, L. Chayes, S.A. Smith, *Random Structures & Algorithms* **31**, 354 (2007)
24. A.K. Hartmann, *The European Physical Journal B* **84**, 627 (2011)
25. A.K. Hartmann, *The European Physical Journal Special Topics* **226**, 567 (2017)
26. A.K. Hartmann, *Big Practical Guide to Computer Simulations* (World Scientific, Singapore, 2015)
27. F. den Hollander, *Large Deviations* (American Mathematical Society, Providence, 2000)
28. H. Touchette, *Physics Reports* **478**, 1 (2009)
29. J. Hopcroft, R. Tarjan, *Commun. ACM* **16**, 372 (1973)
30. T.H. Cormen, C.E. Leiserson, R.L. Rivest, C. Stein, *Introduction to algorithms* (MIT press, 2009)
31. B. Dezső, A. Jüttner, P. Kovács, *Electronic Notes in Theoretical Computer Science* **264**, 23 (2011), proceedings of the Second Workshop on Generative Technologies (WGT) 2010
32. G. Ghoshal, Ph.D. thesis, University of Michigan (2009)
33. M.E.J. Newman, S.H. Strogatz, D.J. Watts, *Phys. Rev. E* **64**, 026118 (2001)
34. H. Klein-Hennig, A.K. Hartmann, *Phys. Rev. E* **85**, 026101 (2012)
35. A.K. Hartmann, *Phys. Rev. E* **65**, 056102 (2002)
36. S. Wolfsheimer, B. Burghardt, A.K. Hartmann, *Algorithms for Molecular Biology* **2**, 9 (2007)
37. P. Fieth, A.K. Hartmann, *Phys. Rev. E* **94**, 022127 (2016)
38. G. Claussen, A.K. Hartmann, S.N. Majumdar, *Phys. Rev. E* **91**, 052104 (2015)
39. T. Dewenter, G. Claussen, A.K. Hartmann, S.N. Majumdar, *Phys. Rev. E* **94**, 052120 (2016)
40. H. Schawe, A.K. Hartmann, S.N. Majumdar, *Phys. Rev. E* **97**, 062159 (2018)
41. H. Schawe, A.K. Hartmann, arXiv preprint arXiv:1808.10698 (2018)
42. A.K. Hartmann, *Phys. Rev. E* **89**, 052103 (2014)
43. A. Engel, R. Monasson, A.K. Hartmann, *Journal of Statistical Physics* **117**, 387 (2004)
44. A.K. Hartmann, M. Mézard, *Phys. Rev. E* **97**, 032128 (2018)
45. F. Wang, D.P. Landau, *Phys. Rev. Lett.* **86**, 2050 (2001)
46. F. Wang, D.P. Landau, *Phys. Rev. E* **64**, 056101 (2001)
47. B.J. Schulz, K. Binder, M. Müller, D.P. Landau, *Phys. Rev. E* **67**, 067102 (2003)
48. R.E. Belardinelli, V.D. Pereyra, *Phys. Rev. E* **75**, 046701 (2007)
49. R.E. Belardinelli, V.D. Pereyra, *The Journal of Chemical Physics* **127**, 184105 (2007)
50. J. Lee, *Phys. Rev. Lett.* **71**, 211 (1993)
51. R. Dickman, A.G. Cunha-Netto, *Phys. Rev. E* **84**, 026701 (2011)
52. B. Efron, *Ann. Statist.* **7**, 1 (1979)
53. A.P. Young, *Everything You Wanted to Know About Data Analysis and Fitting but Were Afraid to Ask*, Springer-Briefs in Physics (Springer International Publishing, 2015), ISBN 978-3-319-19050-1